Int. J. Heat Mass Transfer. Vol. 21, pp. 1185–1196
Pergamon Press Ltd. 1978. Printed in Great Britain

FREEZING–MELTING HEAT TRANSFER IN A TUBE FLOW

A. YIM,* M. EPSTEIN,† S. G. BANKOFF,‡ G. A. LAMBERT and G. M. HAUSER
Argonne National Laboratory,† 9700 South Cass Avenue, Argonne, IL 60439, U.S.A.

(*Received* 9 *November* 1977 *and in revised form* 24 *January* 1978)

Abstract—Consideration is given to the heat-transfer problem involving solidification of a flowing liquid onto a melting wall. In particular, an experimental study of hot Freon 112A (m.p. 40.5°C) in turbulent flow through a thick ice pipe has been carried out. The major emphasis was on the melting attack of the ice pipe wall by the flowing Freon. The effects of both Freon injection pressure and temperature on the amount of melted ice collected at the pipe exit for a fixed injection period were investigated. The shape of the melted ice channel as a function of time, injection pressure and Freon temperature was determined from the frozen Freon "casting" that remained in the ice pipe. Numerical results based on a simple quasi-steady melting model were compared with the experimentally determined ice melting results. The model was found to represent the data reasonably well for Freon temperatures above 70°C, indicating that the ice wall melting process is controlled by the growth and decay of frozen Freon layers on the ice pipe wall.

NOMENCLATURE

a, modified Stanton number: equation (20);
A, Stanton number;
b, modified friction factor; equation (21);
B, phase conversion parameter; equation (11);
c, heat capacity;
C, dimensionless Freon 112A heat capacity; equation (22);
f, coefficient of friction;
h, convective heat-transfer coefficient;
H, latent heat of fusion;
k, thermal conductivity;
K, friction loss coefficient excluding the ice pipe; equation (1);
L, length of ice pipe;
m, mass;
M, dimensionless mass; equations (17), (18);
P_0, Freon injection pressure;
$\dot{q}''$, convective heat flux;
r, local ice pipe radius;
r_0, inlet and exit radius and initial radius of ice pipe; Fig. 10;
R, normalized ice pipe radius;
t, time;
t_{life}, crust lifetime;
T, local temperature of Freon flow;
T_f, temperature within Freon crust;
T_w, temperature within ice melt layer;
T_0, Freon injection temperature; Fig. 10;
T_{mp}, equilibrium melting temperature;
T_i, temperature at Freon crust–ice melt interface; Fig. 9;
u, local axial Freon flow velocity;
u_0, inlet and exit Freon velocity; Fig. 10;
y, distance measured from Freon crust–ice melt interface; Fig. 9;
z, axial coordinate measured from ice pipe inlet; Fig. 10.

Greek symbols

α, thermal diffusivity;
β, dimensionless heat of fusion; equation (A.10);
δ, crust or melt layer thickness;
Δ, dimensionless crust or melt layer thickness; equation (A.8);
θ_i, dimensionless Freon crust–ice melt interface temperature; equation (A.9);
λ, temperature profile shape factor; equation (A.7);
ρ, density;
σ, ρkH ratio; equation (A.10);
τ, dimensionless time; equation (19) or equation (A.9);
χ, temperature profile shape factor; equation (A.6).

Subscripts

1,2, at ice pipe inlet, exit;
f, Freon 112A;
i, ice;
w, ice melt (water).

* Present address: American Can Company, Barrington, Illinois. Based in part on a dissertation submitted to the Faculty of Northwestern University by A. Yim in partial fulfillment of the requirements for the degree of Master of Science (Chemical Engineering) (1977).

† Reactor Analysis and Safety Division; To whom inquiries concerning this paper should be directed.

‡ Present address: Northwestern University, Evanston, Illinois.

1. INTRODUCTION

LAMINAR or turbulent channel flows with phase change at the wall have been studied extensively in the past [1–14]. Most of this work is concerned with the freezing of liquids in channels with emphasis on (i) the shape of the frozen layer and the freezing section pressure drop under steady-state conditions [1–5], (ii) the transient growth of the frozen layer for the case

where a fully developed channel flow is suddenly disturbed by the introduction of a uniform and steady sub-freezing temperature along a certain length of the channel wall [6–9], and (iii) the transient flow and freezing of a liquid at its fusion temperature as it penetrates into an initially empty cold tube [10–13]. Relatively little work has been reported on channel flows with melting at the wall. The problem of melting in laminar flow in a two-dimensional channel was treated theoretically by Boley [14], with the restriction that the meltable wall material be the same as the flow.

A problem of importance to fast nuclear reactor safety studies is the flow of high-temperature molten ceramic fuel (~3000°C) through the steel channels that surround the reactor core. If the initial temperature of the steel channel wall is sufficiently high, the molten ceramic–steel interface temperature falls between the fusion temperatures for these substances upon contact, resulting in solidification in the initially molten ceramic fuel and melting in the initially solid steel wall. This problem is different than the solidification or melting problems mentioned above in that freezing and melting at the channel wall take place simultaneously. Clearly, this freezing–melting process can arise when the hot liquid stream and the channel wall are different materials of immiscible liquids, with the fusion temperature of the hot flowing material exceeding that of the wall material. Any attempt at predicting the melting rate of the channel wall in this situation must include the transient behavior of a growing crust on the wall melt layer. The frozen crust may protect the melting wall from direct contact with the hot channel flow. Alternatively, the superheat of the hot stream and the local heat-transfer rates may be such that the initially formed protective crust is remelted and the wall melt layer becomes exposed to the channel flow and, perhaps, is entrained by the flow. A simple wall melting model that incorporates the growth and remelting of the solidified layer is developed below. Interestingly enough, a frozen layer formed in this manner may be somewhat mobile owing to the underlying layer of wall melt and the fluid frictional shear forces acting on the crust surface.

In [15] an analysis is given of simultaneous solidification and melting heat transfer, but the work centers on the conduction aspects of the problem. A series of tests in which limited quantities of molten uranium dioxide–metallic molybdenum mixture were injected into steel tubes and reactor subassembly channels is reported in [16, 17]. In these tests, a complex two-phase mixture of high-pressure nitrogen gas, 3200°C uranium dioxide and metallic molybdenum was generated by a thermite-type reaction between uranium powder containing some uranium nitride and molybdenum trioxide. Different steel channel wall temperatures were selected and the conditions that resulted in partial or complete ablation of the channel wall were recorded.

To the best of the authors' knowledge, no prior laboratory work has been carried out regarding the heat-transfer characteristics of a freezing liquid flowing through a melting channel other than that reported in [16, 17], and essentially no experimental studies have been made of this process under well-defined flow conditions. The object of this paper is, therefore, to make an experimental study of a tube flow with simultaneous melting and solidification at the tube wall, along with a simple theoretical analysis of this melting–freezing problem for an ideal case. The present study investigated the turbulent flow of hot Freon 112A (m.p. 40.5°C) through a thick ice pipe. The ice pipe was maintained at the melting temperature throughout. The effects of Freon injection pressure and temperature on the amount of melted ice collected at the pipe exit were determined.

2. EXPERIMENTAL APPARATUS

A schematic diagram of the experimental set up is shown in Fig. 1. Briefly, two solenoid valves separated a 150 cm-long, thick-walled ice pipe from a Freon reservoir and a receiving vessel.

A stainless steel vessel made from 6 in schedule 40 pipe (15.41 cm I.D.), approximate capacity of 4000 cm^3, was used as the Freon reservoir. Heating wires were wrapped around the reservoir and insulated with ceramic fiber to bring the Freon to, and maintain

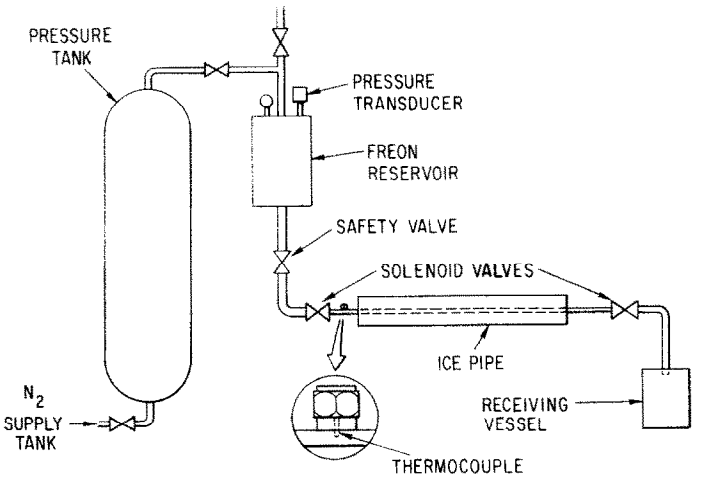

FIG. 1. Schematic diagram of the experimental apparatus.

it at, the desired initial temperature. All temperature measurements were made with 1/16 in (0.16 cm sheathed) chromel–alumel thermocouples. Two thermocouples were located at different levels within the reservoir to check that a uniform temperature was attained prior to a run. The reservoir was connected at the top to a large 3×10^5 cm^3 tank pressurized with nitrogen gas to maintain a constant Freon injection pressure. A pressure transducer was installed in the reservoir and its output was recorded on a Hewlett–Packard strip chart recorder.

A 1/2 in schedule 40 stainless steel pipe (1.6 cm I.D.) connected the reservoir to a 1 in solenoid valve. A 1/2 in ball valve was also installed in this section to allow manual shutoff of the flow in case the ice pipe ruptured. On the downstream side of the solenoid valve, a thermocouple extended into the center of the inlet tube to monitor the Freon flow temperature just prior to entering the ice pipe. This temperature was recorded on the strip chart recorder. Another 1 in solenoid valve controlled the flow from the ice pipe into the receiving vessel. "Nylaflow" (nylon) pressure tubing of 0.749 cm I.D. provided connections between the solenoid valves and the ice pipe entrance and exit.

The ice pipe was cast in a 150 cm-long plexiglass tube of 5.7 cm I.D. (see Fig. 2). Two 0.635 cm-thick

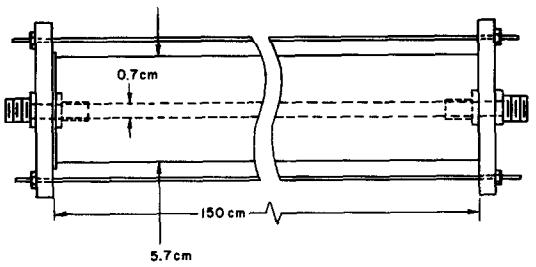

FIG. 2. Schematic diagram of plexiglass ice pipe mold.

plexiglass squares reinforced with 0.16 cm-thick galvanized steel sheets formed the ends of the plexiglass mold. One end was permanently bonded to the tube with epoxy while the other end piece was kept in position by two 0.318 cm-dia threaded steel rods running the length of the ice pipe and a rubber gasket to prevent water leakage. Swagelock nylon bulkhead adaptors of 0.714 cm I.D. were frozen in place in the ice to make the necessary connections to the Nylaflow pressure tubing and the solenoid valves at the inlet and exit sections.

Each ice pipe was made by inserting a 0.635 cm O.D. copper tube coaxially in the plexiglass ice mold tube filled with distilled water. The temperature of the freezer in which the pipes were placed was maintained between -10 and -12°C, and the pipes were allowed to freeze overnight. A slit was cut along the length of the plexiglass tube wall to allow for expansion as the ice froze. Cracks were frequently observed to form in the ice when the freezer temperature was much below -12°C. This in turn led to Freon leaks during the runs and was avoided. After complete solidification, the copper tube was removed by passing hot water (~ 80°C) through the tube for several seconds. This technique resulted in an ice pipe with a smooth inner wall having an inside diameter of 0.7 cm ($r_0 = 0.35$ cm).

All the valves and connecting tubes outside the ice pipe were wrapped with heating wires and were insulated. Provision was also made to measure the temperature of the valves and the walls of the connecting tubes by mounting surface thermocouples at the appropriate locations. This instrumentation assured Freon temperature uniformity between the reservoir and the ice pipe entrance and that the connections between the ice pipe exit and the receiving vessel were maintained above the freezing point of Freon.

3. EXPERIMENTAL PROCEDURE

The reservoir was filled with liquid Freon to a predesignated level using a dipstick to make sure the level was the same for all runs. The liquid Freon in the reservoir and the lines between the reservoir and the ice pipe were preheated to a desired temperature. The exit tubing leading from the ice pipe was always maintained at about 55°C to prevent Freon solidification outside the ice pipe. The valve connecting the reservoir to the nitrogen pressure tank was opened and the pressure level adjusted. The ice pipe was placed into a galvanized box with a plexiglass cover as a safety measure in case of ice rupture. The necessary connections were made between the ice pipe fittings and the Freon inlet and exit flow lines.

Each run was started by activating the two solenoid valves simultaneously for a preset duration (set on a timer) and thereby allowing the hot Freon to enter the ice pipe. The Freon was allowed to flow through the ice pipe and into the receiving vessel for a period of 6–11 s depending on the injection pressure, at which time the solenoid valves were closed simultaneously and the Freon flow shutoff. At the end of each run the Freon and the melted ice collected in the receiving vessel were separated and their individual masses were recorded.* The shape of the melted ice channel was determined from the frozen Freon "casting" that remained in the ice pipe (i.e. trapped between the two solenoid valves). This was done by allowing the ice to melt and measuring the radial dimensions of the frozen Freon at several axial positions.

To test out the system and to determine the overall friction loss coefficient for the flow system excluding the ice pipe, K, as well as the delay time associated with opening and closing of the solenoid valves, a series of experiments were run without the ice pipe in position. The procedure was identical as that described for the runs made with the ice pipe except that the ice pipe inlet and outlet lines were connected with a Swagelock union. The amount of Freon collected in the receiving vessel, m_f, for a given inlet Freon temperature and reservoir pressure was plotted as a function of the injection period set on the solenoid valve timer. This is

*The Freon 112A-water system is an immiscible material pair.

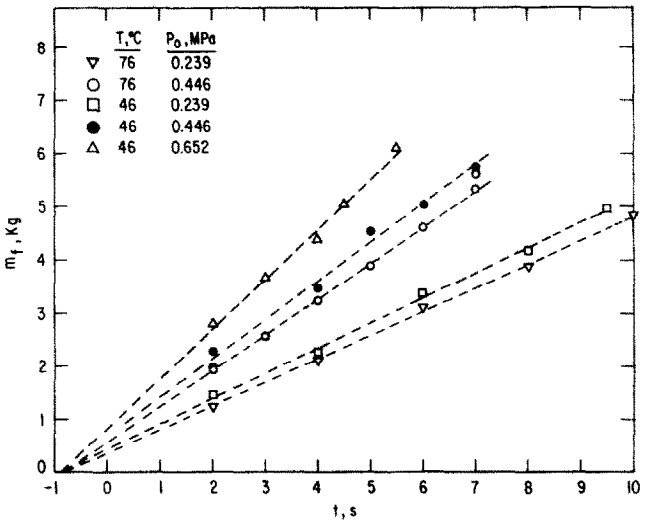

FIG. 3. Calibration of valve delay time and determination of K, the overall friction loss coefficient excluded.

shown in Fig. 3. By "visually fitting" straight lines through the data points obtained and extrapolating to $m_f = 0$, the intercept on the abcissa gave the magnitude of the valve delay time. This was repeated for different injection pressures and Freon temperature and the average value of the delay time was found to be 0.8 s. The "negative delay time" indicated in Fig. 3 implies that the time to close the valves exceeds the time to open the valves. The delay time is added to that set on the valve timer to determine approximately the injection period. Since the flow is highly turbulent, the pressure drop external to the ice pipe is assumed to be well represented by

$$\Delta P_{ext} = \tfrac{1}{2} K \rho_f u_0^2 \tag{1}$$

where r_0 is the radius of the inlet tube ($r_0 = 0.357$ cm).* velocity in the nylon tube leading into the ice pipe (when the ice pipe is in place). In the absence of the ice pipe, the total amount of Freon collected is simply

$$m_f = \pi r_0^2 \rho_f u_0 t \tag{2}$$

where r_0 is the radius of the inlet tube ($r_0 = 0.357$ cm).* Eliminating u_0 between the above two equations and solving for K, we obtain

$$K = 2\pi^2 r_0^4 \rho_f \Delta P_{ext} (t/m_f)^2. \tag{3}$$

From Fig. 3 it is found that K varies in the range 3.1–3.7.

4. EXPERIMENTAL RESULTS

The first set of runs were carried out with the Freon reservoir temperature, T_0, held approximately constant at 91.0°C and the reservoir pressure, P_0, varied from 0.17 MPa (~1.7 atm) to 0.635 MPa (~6.35 atm). In the second set of runs, P_0 was held constant at 0.446 MPa (~4.46 atm) and T_0 varied from 45 to 91°C. In all the runs, the ice pipes were maintained at a uniform temperature between 0 and −3°C to ensure that the desired condition of simultaneous ice wall melting and Freon crust formation upon contact was achieved.

Photographs of the ice pipe entrance region before and after Freon is allowed to pass through the ice section are shown in Fig. 4 for an injection period of 6.8 s, $P_0 = 0.515$ MPa and $T_0 = 90$°C. Note that the frozen Freon casting remaining in the ice pipe channel has a milky white appearance. Freon 112A in the liquid state is a clear fluid. As a result of this color change upon freezing, the Freon crust behavior during a run was visible through the ice pipe wall.†

At high injection pressures and temperatures, the inner ice wall appears to be partially covered by a random array of Freon crust "spots". The spots seem to be slightly elongated in the direction of flow. The crust spots are not permanent, but disappear and sometimes are replaced by a new spot that grows at the same site. The departure or disappearance of crust spots is attributed to a combination of crust melting (see Section 6) and crust mobility owing to the underlying layer of melted ice. At lower pressures and/or temperatures, sections of Freon crust were clearly seen to move or slide along the ice pipe wall in the direction of flow with a jerking motion on a stop and go basis. At times, the crust sections were observed to accumulate in the exit region of the ice pipe right in front of the exit tube (exit bulkhead adapter) forming a Freon "crust jam", as illustrated schematically in Fig. 5. For some runs performed at low initial Freon temperatures ($T_0 \lesssim 70$°C), tiny solid Freon particles were seen flowing into the receiving vessel. This Freon "hail" may be caused by turbulent mixing between the relatively cold melted ice and the flowing Freon. Perhaps some of the melted ice in the form of water droplets is rapidly entrained by the bulk Freon flow.

*The mold for forming the ice pipe cavity was such that the resulting ice channel radius $r_0 = 0.35$ cm was 0.007 cm less than the radius of the nylon inlet (or exit) tube. This difference is ignored in the theoretical part of the paper presented in Section 5.

†The opaqueness of solid Freon 112A is probably a result of the formation of small air bubbles upon freezing.

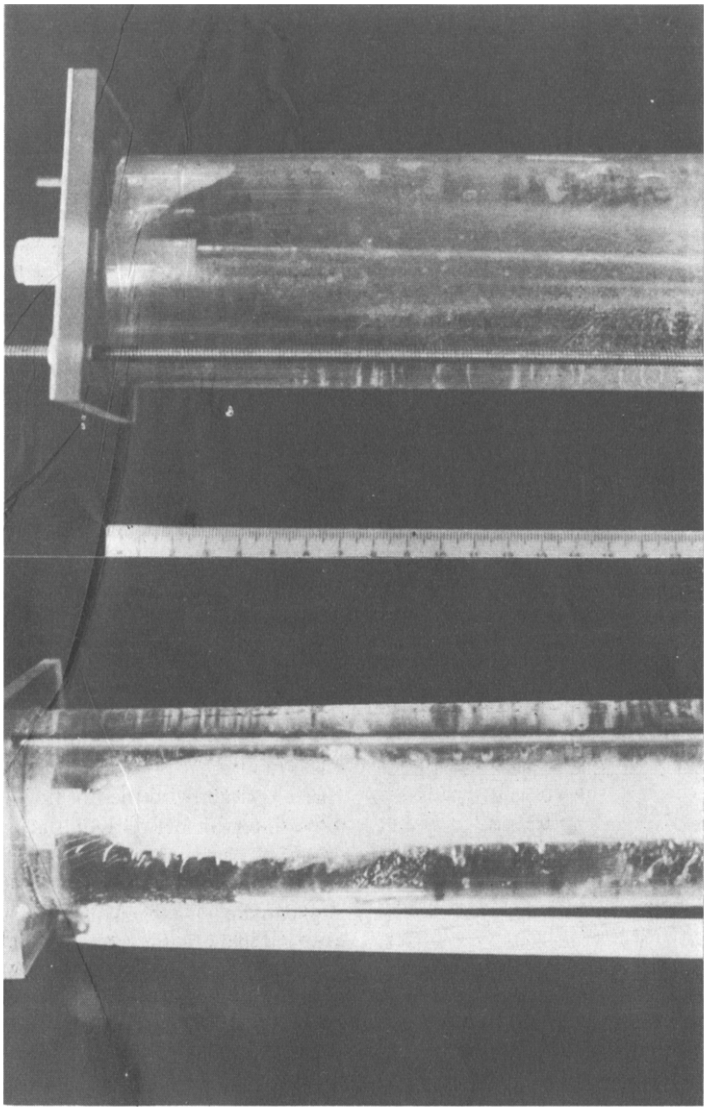

FIG. 4. (a) Entrance region of ice pipe at $t = 0$. (b) Entrance region of ice pipe after Freon 112A solidification. ($P_0 = 0.515$ MPa, $T_0 = 90°C$, $t = 6.8$ s.)

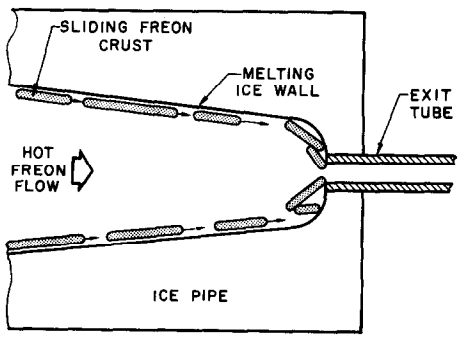

FIG. 5. Pictorial representation of Freon crust motion and jamming in the exit region of the melting ice pipe.

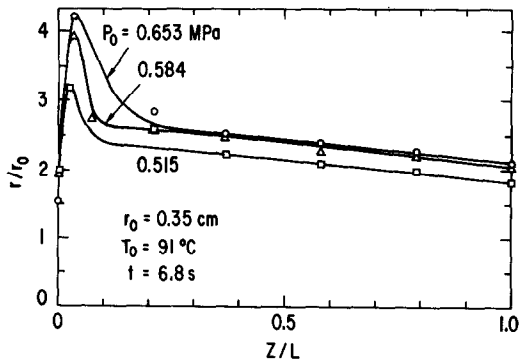

FIG. 6. The effect of injection presure on the measured ice pipe profile.

The entrained water droplets then serve as sites for Freon solidification into particles. Such an ablation-induced bulk freezing mechanism was first postulated in [16] for the UO_2-steel system. The use of a 150 cm-long ice pipe allowed our experiment to also deal with the question of bulk freezing as a mechanism for flow blockage. It was suggested in [16] that as a result of turbulent mixing between the relatively cold melted

channel wall material and the hot stream, a freeze blockage might occur in the region just behind the advancing flow front (during the early stages of the transient before the flow traverses the axial length of the channel). Freon is predicted to penetrate only ~80 cm into the ice pipe before it gives up its latent heat of fusion to the entrained ice melt and thereby causes the flow to stop (see equation (31) of [16]). This type of freeze blockage was not observed here as the Freon always emerged from the ice pipe exit section.

The observed shapes of the melted ice channel as a function of injection pressure, initial Freon temperature and injection period are shown in Figs. 6, 7 and 8, respectively. In most cases the channel radius increases in the inlet region and passes through a maximum value at an axial location of $z/L \sim 0.03$. Thereafter, the radius decreases and the channel profile becomes linear beyond $z/L \sim 0.2$. This channel profile "bulge" in the ice pipe entrance region can be seen in Fig. 4 and, presumably, is due to the thermal entrance region effect for developed turbulent flow.

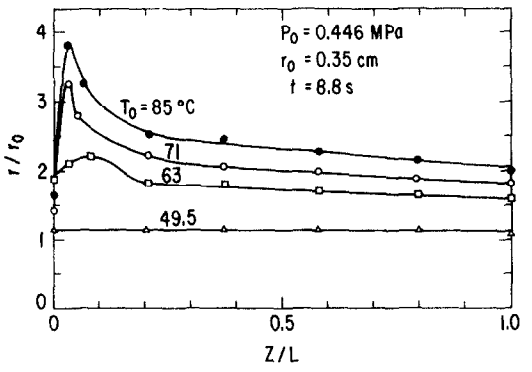

FIG. 7. The effect of Freon temperature on the measured ice pipe profile.

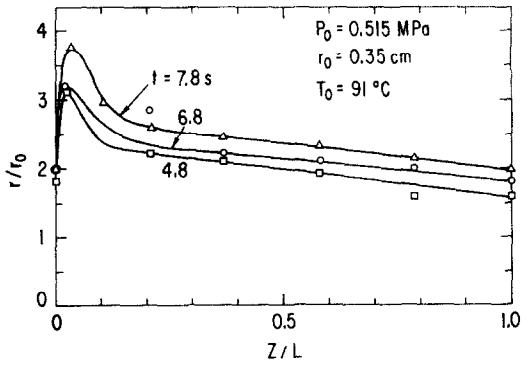

FIG. 8. The effect of injection period on the measured ice pipe profile.

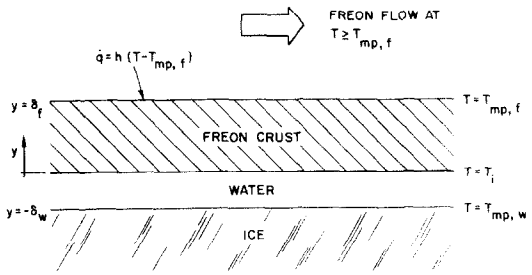

FIG. 9. Postulated simultaneous ice wall melting and Freon crust formation.

5. ANALYSIS

The problem of predicting the average melting rate for the ice pipe wall is complicated by the fact that we must deal with the transient behavior of a growing Freon crust on the melting ice wall together with a time dependent Freon flow rate due to the melting process. If it is assumed that the Freon flow is quasi-steady and if the Freon crust motion (sliding) is ignored, then the problem is greatly simplified.

Initially the ice pipe wall is at its freezing temperature. Thus, when Freon flow commences a Freon crust will build up on the melting ice wall, as sketched in Fig. 9. The growth of the Freon crust comes to a stop when the conduction heat flux into the melting ice layer balances convection from the Freon flow. Then the frozen Freon layer will begin to melt; it ultimately disappears when melting is complete. We assume that at this instant the exposed water layer is removed (entrained) by the highly turbulent Freon flow and the process of Freon crust growth and decay begins again. This implies that, except for the short period of time during which the melted ice is removed from the wall, the Freon crust protects the melting ice surface from direct contact with the hot flowing Freon melt. If the time interval between initial growth to complete removal of the crust (crust lifetime, t_{life}) is small in comparison with the Freon injection period, ice melting can be visualized as a process in which ice is continuously being removed (ablated) at a rate proportional to the difference between the local Freon flow temperature and the Freon fusion temperature, $T - T_{mp,f}$. In particular, we postulate that the instantaneous rate of ice wall erosion is approximately equal to the mass of the ice melt layer at the moment the protective Freon crust is melted away, $\rho_i \delta_w(t_{life})$, divided by the Freon crust lifetime, t_{life}.

In addition to the above idealization the following assumptions are made:

1. The flow is highly turbulent and the local heat-transfer coefficient at the Freon melt–crust interface, h, can be represented by the constant Stanton number formula:*

$$\frac{h}{c_f \rho_f u} = A = 8 \times 10^{-4}. \tag{4}$$

2. All physical properties are constant, and the properties of liquid and solid Freon 112A are taken to be the same.

3. During the period t_{life}, the solidified Freon layer and the trapped ice melt layer are thin compared with the local channel radius so that curvature effects in the crust and in the melt layer may be neglected.

4. The crust lifetime is sufficiently short so that the local flow temperature and convective heat-transfer coefficient remain essentially constant during each

* A is a function of the Prandtl number. The value given here is for Freon 112A ($Pr \simeq 9.6$).

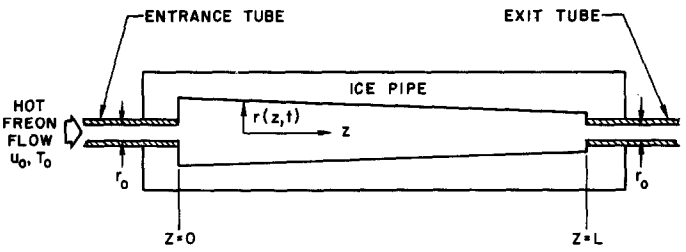

FIG. 10. Idealized melting ice pipe.

growth and decay period of the frozen Freon crust.

5. In the Freon crust and in the wall melt layer conduction takes place in the radial direction only.

6. Frictional resistance to flow in the ice pipe at the Freon melt–crust interface can be represented by the shear stress formula

$$\tau = \tfrac{1}{2} f \rho_f u^2 \tag{5}$$

where f, the friction factor, is assumed constant ($f = 0.005$).

7. The Freon melt flow is in the axial direction only and the velocity profile is flat.

8. The exchange of liquid enthalpy due to turbulent mixing between the flowing Freon and entrained melted ice is ignored.

9. The thermal entrance region is not taken into account.

10. The ice pipe profile $r(z,t)$ is a slowly varying linear function of the axial position z, as shown in Fig. 10.

11. Pressure drops due to expansion and contraction that develop in the inlet and exit regions of the ice pipe as the melting process progresses are neglected.

12. The group $[LA\rho_f c_f (T_0 - T_{mp,f})/(r_0 \rho_i H_i)]$ is much less than unity.

13. The time required for the Freon flow to fill the pipe is small compared with the injection period.

The problem of a frozen layer in convective flow growing on a melting solid was studied analytically (see Appendix) and the results confirm the validity of assumptions 3 and 4 for sufficiently high local Freon flow velocities and temperatures. As a result of assumption 12, which may be shown to be equivalent to the assumption of negligible mass and thermal inertia in the hot Freon flow, the transient term in the energy equation may be neglected and the momentum equation is simply a balance of the pressure gradient with frictional resistance in the Freon flow. Assumption 8 comes from the experimental observation that the mass ratio of melted ice to Freon collected in the receiving vessel is small ($m_w/m_f \lesssim 0.06$). Assumption 10 is also based on experimental observation (see Section 5).* Some errors are introduced by neglecting variations in the Stanton number A and in the friction factor f as the local channel radius increases due to melting and by ignoring the thermal entrance region [see assumptions (1), (6) and (9)]; however, even an approximate allowance for these effects would greatly increase the complexity of the computational task. Moreover, in view of the lack of information regarding Freon crust behavior on melting ice, such an analysis is probably not justified.

For the model of the melting ice pipe shown in Fig. 10 and under the assumptions listed above, the governing equations are:

$$u_0(t) r_0^2 = u(z,t) r^2(z,t)$$

(continuity for the Freon) (6)

a mechanical energy balance for the flow system composed of inlet and exit piping, valves, and the ice pipe [see equation (1)]

$$\Delta P = \tfrac{1}{2} K \rho_f u_0^2(t) + f \rho_f \int_0^L \frac{u^2(z,t)}{r(z,t)} \, dz \tag{7}$$

and a thermal balance on the flowing Freon which equates the heat leaving through the frozen Freon layer at the wall to the decrease of enthalpy of the hot Freon stream

$$[T(z,t) - T_{mp,f}] h \partial z = -\tfrac{1}{2} c_f \rho_f u r \partial T(z,t). \tag{8}$$

The local heat lost from the hot Freon crust during the crust lifetime, $\dot{q}'' t_{\text{life}} = h(T - T_{mp,f}) t_{\text{life}}$, must equal the sensible heat stored in the underlying melted ice layer plus the heat required to produce the ice layer:

$$\dot{q}'' t_{\text{life}} = \rho_w c_w \int_{-\delta_w(t_{\text{life}})}^{0} [T_w(t_{\text{life}}) - T_{mp,w}] \, dy + \rho_i H_i \delta_w(t_{\text{life}}) \tag{9}$$

where $\delta_w(t_{\text{life}})$ is the ice melt layer thickness at the instant the Freon crust is completely melted away and y is the distance measured from the Freon crust–melted ice interface (see Fig. 9). Equation (9) follows from assumptions 3–5. We suppose that a linear temperature profile exists through the ice melt layer. Substituting this profile into the integral in equation (9), we obtain

$$\dot{q}'' t_{\text{life}} = B \rho_i H_i \delta_w(t_{\text{life}}) \tag{10}$$

*The validity of the linear ice profile assumption can be rigorously demonstrated (Condiff and Epstein, in preparation).

where B, the phase conversion parameter, is given by*

$$B \equiv 1+\tfrac{1}{2}\frac{\rho_w c_w(T_{mp,f}-T_{mp,w})}{\rho_i H_i}. \tag{11}$$

From the relation between the ice melting rate, $\rho_i\delta_w(t_{life})/(t_{life})$, and the rate of change of the local ice pipe radius r, namely

$$\frac{\rho_i\delta_w(t_{life})}{t_{life}} = \rho_i\frac{\partial r}{\partial t} \tag{12}$$

we have

$$BH_i\rho_i\frac{\partial r}{\partial t} = \dot{q}'' = h(T-T_{mp,f}). \tag{13}$$

The instantaneous mass velocity of the hot Freon stream is

$$\frac{dm_f}{dt} = \pi r_0^2\rho_f u_0 \tag{14}$$

and the flow rate of melted ice pipe material at the pipe exit is given by

$$\frac{dm_w}{dt} = 2\pi\rho_i\int_0^L r\frac{dr}{dt}\,dz. \tag{15}$$

Finally, the experimentally determined pipe radius profile suggests the following simple linear relation for $r(z,t)$:

$$\frac{r(z,t)}{r_0} = R_1(t)+[R_2(t)-R_1(t)]\frac{z}{L} \tag{16}$$

where $R_1(t)$ is simply the (normalized) instantaneous ice pipe radius at the inlet location $\{R_1(t)=r(0,t)/r_0\}$ and $R_2(t)$ is the instantaneous pipe radius at the exit $[R_2(t)=r(L,t)/r_0]$.

It is now convenient to introduce the following set of dimensionless variables and parameters:

$$M_f \equiv \frac{Ac_f(T_0-T_{mp,f})}{\pi\rho_i r_0^3 H_i B}m_f$$

(dimensionless Freon mass) (17)

$$M_w \equiv \frac{Ac_f(T_0-T_{mp,f})}{\pi\rho_i r_0^3 H_i B}m_w$$

(dimensionless ice melt mass) (18)

$$\tau \equiv \frac{Ac_f\rho_f(T_0-T_{mp,f})}{BH_i\rho_i r_0}\left(\frac{2\Delta P}{K\rho_f}\right)^{1/2}t$$

(dimensionless time) (19)

$$a \equiv \frac{2AL}{r_0}$$ (modified Stanton number) (20)

$$b \equiv \frac{fL}{2r_0K}$$ (modified friction factor) (21)

$$C \equiv \frac{c_f(T_0-T_{mp,f})}{BH_i}$$

(dimensionless Freon heat capacity). (22)

*For the Freon 112A–ice system, equation (11) gives $B = 1.25$. The results of a detailed analysis of this conduction problem which attempts to obtain the correct nonlinear temperature distribution (see Appendix) show that the more correct value of B is around 10% lower than this. Temperature profile distortion within the ice melt layer will be more important in applications where the melt liquid superheat is high or more precisely for values of $B \gtrsim 1.5$.

Then, from equations (4), (6)–(8) and equations (13)–(16), the following system of dimensionless equations is obtained

$$R_1^2\frac{dR_1}{d\tau} = \left|1+b\frac{R_2^{-4}-R_1^{-4}}{R_1-R_2}\right|^{1/2} \tag{23}$$

$$\frac{dR_2}{d\tau} = \left(\frac{R_1}{R_2}\right)^{2-a(R_1-R_2)}\frac{dR_1}{d\tau} \tag{24}$$

$$\frac{dM_f}{d\tau} = R_1^2\frac{dR_1}{d\tau} \tag{25}$$

$$\frac{dM_w}{d\tau} = C[1-(R_2/R_1)^{a(R_1-R_2)}]\frac{dM_f}{d\tau}. \tag{26}$$

Equations (23)–(26) are sufficient to determine the four coupled unknown functions R_1, R_2, M_f, and M_w subject to the initial conditions $R_1 = R_2 = 1.0$ and $M_f = M_w = 0$ when $t = 0$. Equations (23) and (24) are obtained by substituting the ice channel profile expression, equation (16), into equation (13) and evaluating the result at $z = 0$ and $z = L$. Equations (23)–(26) were integrated numerically. In order to start the integration for τ near zero, short-time solutions are required. These are

$$R_1 = 1+(1+b)^{-1/2}\tau+\ldots \tag{27}$$

$$R_2 = 1+e^{-a}(1+b)^{-1/2}\tau+\ldots \tag{28}$$

$$M_f = (1+b)^{-1/2}\tau+\ldots \tag{29}$$

$$M_w = C(1+e^{-a})(1+b)^{-1/2}\tau+\ldots. \tag{30}$$

6. DISCUSSION

In Fig. 11, the actual amount of water (ice melt) collected, m_w, as a function of injection pressure is

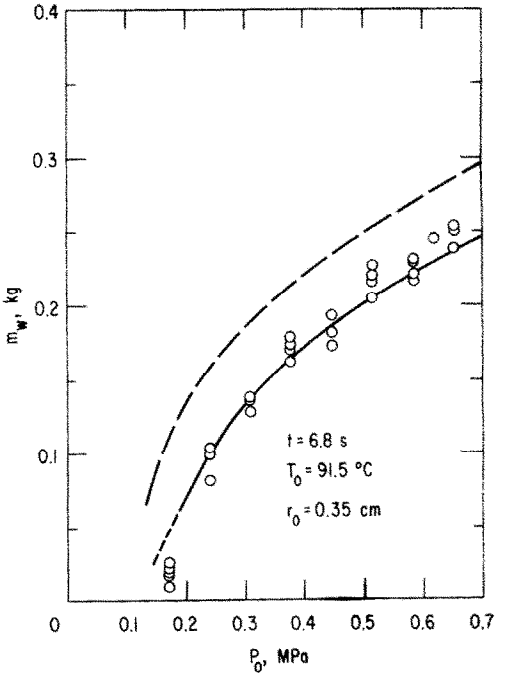

FIG. 11. Mass of melted ice collected vs injection pressure. The dashed line is based on predicted Freon flow rates. The solid line is based on the observed amount of Freon collected.

compared with the theory (dashed curve). Although equations (23)–(26) predict the trend, they overestimate the actual melting results by 15–100% depending upon the value of P_0. Possible sources of error include the assumptions of constant friction factor f and Stanton number A. Since the local ice pipe radius increases with time, these values may increase by as much as 25% during the course of a run. However, it is presently felt that the difference between the test results and the theory can be largely attributed to increased Freon flow resistance as a result of Freon crust motion and buildup in the exit region of the ice pipe (see Section 4). The results shown in Fig. 12 for the mass of Freon collected, m_f, bears this out. The actual amount of Freon collected for every run is considerably less than that predicted (dashed curve). From the results of the analysis, it is found that the amount of Freon collected is insensitive to variations in A or f since, after a short initial period, the computed pressure drop across the melting ice pipe is small compared with the external pressure drop $1/2\ K\rho u_0^2$ [see equation (1)]. Values of K from 5 up to ~18 depending on P_0 were chosen to force the theoretical values of m_f to agree with the experimental values (solid curve in Fig. 12).*

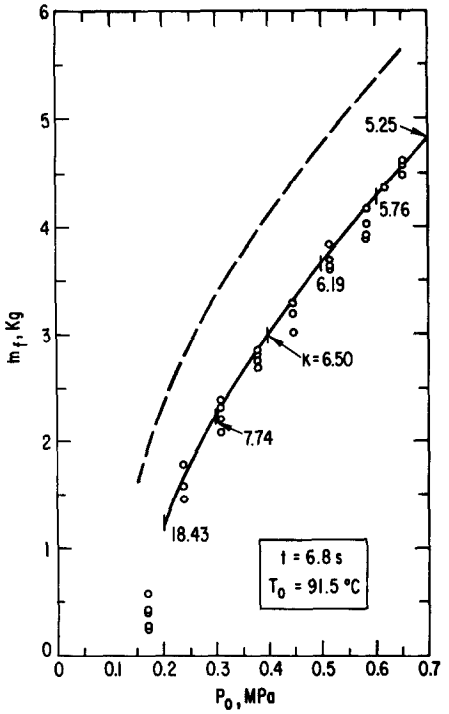

FIG. 12. Mass of Freon 112A collected vs injection pressure. The dashed line represents the theory. The solid line indicates the values of K required to match the measurements.

This resulted in good agreement between the theory and the experimental data for m_w as shown in Fig. 11

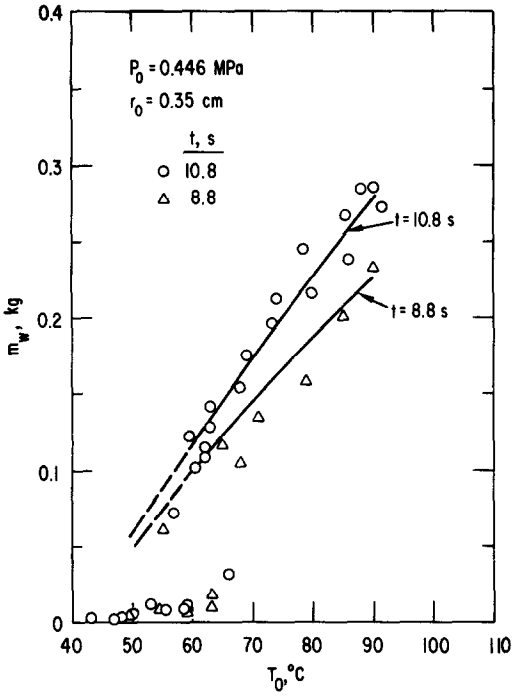

FIG. 13. Mass of melted ice collected vs injection temperature. Solid lines represent predictions based on the observed amount of Freon collected.

(solid curve) and hence the model can be used to estimate average melting rates when the flow velocity is specified. Along the dashed portion of the lower curve in Fig. 11 the Freon crust lifetime, t_{life}, is predicted to be of the order of or exceed the injection period (see Appendix) and, therefore, the major underlying assumption $t \ll t_{life}$ breaks down.

The variation of m_w with initial Freon flow temperature, T_0, for different injection periods is shown in Fig. 13. The experimental data exhibit considerable scatter for $55 < T_0 < 70$°C, with the experimental points essentially divided between an upper and a lower curve. The sudden drop in m_w as T_0 falls below ~70°C is attributed to relatively rapid accumulation of Freon crust in the ice pipe exit region. Observations made through the ice pipe wall during the experiments seemed to support this. The solid curves in Fig. 13 represent the predicted amount of ice melt collected based on the observed amount of Freon collected (see Fig. 14). The Freon flow rate was computed from the theory with $K = 6.3$ to match the measurements for m_f shown in Fig. 14.

7. CONCLUSIONS

In the flow of hot Freon 112A (m.p. 40.5°C) through a melting ice pipe, two distinct modes of Freon freezing were observed. First, sections of Freon crust are formed on the inner melting ice wall. The crust sections are not stationary, but slide over the melting ice with a jerking motion in the direction of flow and, ultimately, may disappear due to remelting. Second, the appearance of small solid Freon particles entering the receiving vessel indicates that melted ice in the form of

*Assuming that the Freon crust jam at the pipe exit can be represented as a thin obstacle with a hole in the middle (or orifice), the extent of this partial flow blockage in terms of flow cross-section (or necking down) is estimated to be a 20% reduction in channel radius for $K = 5$ and a 40% reduction in channel radius for $K = 18$.

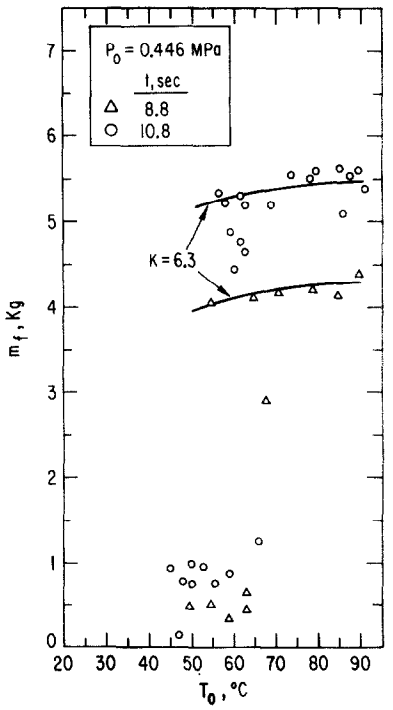

FIG. 14. Mass of Freon 112A collected vs injection temperature. Solid lines indicate the value of K required to match the data.

water droplets act as sites for freezing Freon in the turbulent core.

The Freon 112A flow rate is difficult to predict as a result of the accumulation of frozen Freon skin in the exit region of the ice pipe. The average ice wall melting rate may be predicted by using the experimentally observed average Freon flow rate and by assuming that the melting process is controlled by the growth and remelting of the Freon crust sections on the ice pipe wall.

Acknowledgement—This work was performed under the auspices of the U.S. Energy Research and Development Administration.

REFERENCES

1. R. D. Zerkle and J. E. Sunderland, The effect of liquid solidification in a tube upon laminar-flow heat transfer and pressure drop, *J. Heat Transfer* **90C**, 183–190 (1968).
2. J. C. Mulligan and D. D. Jones, Experiments on heat transfer and pressure drop in a horizontal tube with internal solidification, *Int. J. Heat Mass Transfer* **19**, 213–218 (1976).
3. C. A. Depew and R. C. Zenter, Laminar flow heat transfer and pressure drop with freezing at the wall, *Int. J. Heat Mass Transfer* **12**, 1710–1714 (1969).
4. N. DesRuisscaux and R. D. Zerkle, Freezing of hydraulic systems, *Can. J. Chem. Engng* **47**, 233–237 (1969).
5. A. A. Shibani and M. N. Ozisik, A solution of freezing of liquids of low Prandtl number in turbulent flow between parallel plates, *J. Heat Transfer* **99C**, 20–24 (1977).
6. M. N. Ozisik and J. C. Mulligan, Transient freezing of liquids in forced flow inside circular tubes, *J. Heat Transfer* **91C**, 385–391 (1969).
7. J. A. Bilenas and L. M. Jiji, Variational solution of axisymmetric fluid flow in tubes with surface solidification, *J. Franklin Inst.* **289**, 265–279 (1970).
8. M. H. Chun, R. D. Gasser, M. S. Kazimi, T. Ginsberg and O. C. Jones, Jr., Dynamics of solidification of flowing fluids with applications to LMFBR post-accident fuel relocation, in *Proceedings of the International Meeting on Fast Reactor Safety and Related Physics*, Vol. IV, Conference No. 761001, pp. 1808–1818, Chicago, Illinois (5–8 October 1976).
9. E. P. Martinez and R. T. Beaubouef, Transient freezing in laminar tube flow, *Can. J. Chem. Engng* **50**, 445–449 (1972).
10. F. B. Cheung and L. Baker, Jr., Transient freezing of liquids in tube flow, *Nucl. Sci. Engng* **60**, 445–449 (1972).
11. J. Madejski, Solidification in flow through channels and into cavities, *Int. J. Heat Mass Transfer* **19**, 1351–1356 (1976).
12. M. Epstein, A. Yim and F. B. Cheung, Freezing-controlled penetration of a saturated liquid into a cold channel, *J. Heat Transfer* **99C**, 233–238 (1977).
13. M. Epstein and G. M. Hauser, Freezing of an advancing tube flow, *J. Heat Transfer* **99C**, 687–689 (1977).
14. W. W. Boley, Two dimensional melting in a channel, Ph.D. Thesis, University of Connecticut (1965).
15. M. Epstein, Heat conduction in the UO_2-cladding composite body with simultaneous solidification and melting, *Nucl. Sci. Engng* **51**, 84–87 (1973).
16. M. Epstein, M. A. Grolmes, R. E. Henry and H. K. Fauske, Transient freezing of a flowing ceramic fuel in a steel channel, *Nucl. Sci. Engng* **61**, 310–323 (1976).
17. M. Epstein, R. E. Henry, M. A. Grolmes, H. K. Fauske, G. T. Goldfuss, D. J. Quinn and R. L. Roth, Analytical and experimental studies of transient fuel freezing, in *Proceedings of the International Meeting on Fast Reactor Safety and Related Physics*, Vol. IV, pp. 1788–1798, Conference No. 761001, Chicago, Illinois (5–8 October 1976).
18. R. G. Deissler, Analysis of turbulent heat transfer, mass transfer, and friction factor of smooth tubes at high Prandtl and Schmidt numbers, NACA Report No. 1210 (1955); also, see R. B. Bird, W. E. Stewart and E. N. Lightfoot, *Transport Phenomena*, p. 402, John Wiley, New York (1960).
19. M. Epstein, The growth and decay of a frozen layer in forced flow, *Int. J. Heat Mass Transfer* **19**, 1281–1288 (1976).

APPENDIX

The purpose of this appendix is to treat the problem of the unsteady growth and decay of a frozen layer in a liquid (Freon 112A) flowing past a plane melting (ice) wall. The formulation is based on the integral (profile) method and parallels that of [19] for the behavior of a frozen layer on a non-melting wall. A hot liquid at a bulk temperature T above its solidification temperature $T_{mp,f}$ suddenly flows over a thick cold wall of different material at its melting temperature $T_{mp,w}$ ($T_{mp,f} > T_{mp,w}$). The hot liquid flow–wall interface temperature falls between $T_{mp,f}$ and $T_{mp,w}$ resulting in solidification in the liquid flow and melting in the initially solid wall. In particular, at time zero, a solidification front appears at the plane of separation $y = 0$ and moves in the positive y-direction into the liquid; similarly, a melting front appears at $y = 0$ and moves in the negative y-direction into the solid (see Fig. 9). Of course, this semi-infinite composite region model can be applied to the melting ice pipe problem only when the ice melt layer proceeds a relatively short distance into the wall and the Freon crust thickness is thin on the scale of the channel radius.

Subject to assumptions 1–5 of Section 5, the heat balance conditions at the solidification front ($y = \delta_f$), at the solidified layer–wall melt layer interface ($y = 0$), at the melt front ($y = -\delta_w$), and across the solidified layer and melt layer suffice to provide the desired relationships $\delta_f(t)$ and $\delta_w(t)$. These

conditions are:

$$\rho_f H_f \frac{d\delta_f}{dt} = k_f\left(\frac{\partial T_f}{\partial y}\right)_{y=\delta_f} - h(T - T_{mp}) \quad (A.1)$$

$$k_f\left(\frac{\partial T_f}{\partial y}\right)_{y=0} = k_w\left(\frac{\partial T_w}{\partial y}\right)_{y=0} \quad (A.2)$$

$$\rho_i H_i \frac{d\delta_w}{dt} = k_w\left(\frac{\partial T_w}{\partial y}\right)_{y=-\delta_w} \quad (A.3)$$

a macroscopic heat balance across the solidified layer (Freon crust)

$$\frac{d}{dt}\int_0^{\delta_f} T_f(y,t)\,dy = \alpha_f\left(\frac{\partial T_f}{\partial y}\right)_{y=\delta_f} - \alpha_f\left(\frac{\partial T_f}{\partial y}\right)_{y=0} + T_{mp}\frac{d\delta_f}{dt} \quad (A.4)$$

and a macroscopic heat balance across the wall melt layer (water layer)

$$\frac{d}{dt}\int_{-\delta_w}^{0} T_w(y,t)\,dy = \alpha_w\left(\frac{\partial T_w}{\partial y}\right)_{y=0} - \alpha_w\left(\frac{\partial T_w}{\partial y}\right)_{y=-\delta_w} + T_{mp,w}\frac{d\delta_w}{dt}. \quad (A.5)$$

Equations (A.1)–(A.5) constitute five conditions which the temperature profiles must satisfy. If we assume second-order polynomials for the temperature distributions $T_f(y,t)$ and $T_w(y,t)$, they take the forms

$$\frac{T_f(y,t) - T_{mp,f}}{T_i(t) - T_{mp,f}} = \chi(t)\left[1 - \frac{y}{\delta_f(t)}\right] + [1-\chi(t)]\left[1 - \frac{y}{\delta_f(t)}\right]^2 \quad (A.6)$$

$$\frac{T_w(y,t) - T_{mp,w}}{T_i(t) - T_{mp,w}} = \lambda(t)\left[1 + \frac{y}{\delta_w(t)}\right] + [1-\lambda(t)]\left[1 + \frac{y}{\delta_w(t)}\right]^2 \quad (A.7)$$

where $\chi(t)$ and $\lambda(t)$ are shape functions eliminated in the course of the analysis in favor of the remaining dependent variables. In writing equations (A.6) and (A.7) we have already invoked the condition of temperature continuity at $y = 0$: $T_f(0,t) = T_w(0,t) = T_i(t)$, where $T_i(t)$ is the instantaneous temperature at the frozen layer–wall melt interface.

The following dimensionless variables and parameters will now be introduced:

$$\Delta_f \equiv \frac{h(T - T_{mp,f})}{k_f(T_{mp,f} - T_{mp,w})}\delta_f, \qquad \Delta_w \equiv \frac{h(T - T_{mp,f})}{k_w(T_{mp,f} - T_{mp,w})}\delta_w \quad (A.8)$$

$$\theta_i \equiv \frac{T_i - T_{mp,w}}{T_{mp,f} - T_{mp,w}}, \qquad \tau \equiv \frac{h^2(T - T_{mp,f})^2}{\rho_f H_i k_f (T_{mp,f} - T_{mp,w})}t \quad (A.9)$$

$$\sigma \equiv \frac{\rho_f k_f H_i}{\rho_i k_w H_w}, \quad \beta_f \equiv \frac{H_i}{c_f(T_{mp,f} - T_{mp,w})}, \quad \beta_w \equiv \frac{H_w}{c_w(T_{mp,f} - T_{mp,w})}. \quad (A.10)$$

Then, from equations (A.1)–(A.7), the following system of dimensionless equations is obtained

$$\frac{d\Delta_f}{d\tau} = \frac{\chi(1-\theta_i)}{\Delta_f} - 1 \quad (A.11)$$

$$\frac{d\Delta_w}{d\tau} = \frac{\sigma\lambda\theta_i}{\Delta_w} \quad (A.12)$$

$$\frac{d}{d\tau}[(2+\chi)\Delta_f(1-\theta_i)] = \frac{12\beta_f(1-\theta_i)(1-\chi)}{\Delta_f} \quad (A.13)$$

$$\frac{d}{d\tau}[(2+\chi)\Delta_w\theta_i] = \frac{12\beta_w\sigma\theta_i(1-\lambda)}{\Delta_w} \quad (A.14)$$

$$\frac{(2-\chi)(1-\theta_i)}{\Delta_f} = \frac{(2-\lambda)\theta_i}{\Delta_w}. \quad (A.15)$$

It can be shown that Δ_f, Δ_w, χ, λ, and θ_i can each be represented by a power series of the form

$$\sum_{n=1}^{\infty} a_n \tau^{n/2};$$

however, this series can only be used for short times (as τ increases the series ceases to converge). Therefore, equations (A.11)–(A.15) were converted to an equivalent coupled system of first order ordinary differential equations, which were integrated in the forward direction using the power series solutions to obtain the correct starting behavior. The accuracy of the integral method exploited here has been demonstrated in [19] for a closely related conduction problem and need not be belabored here.

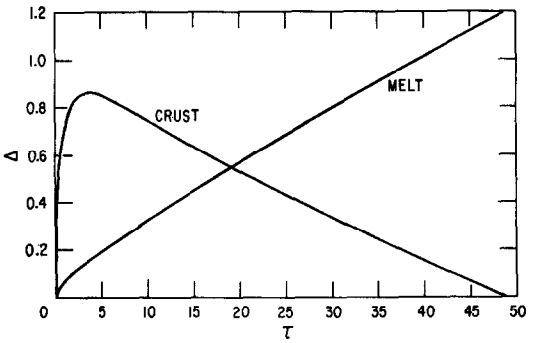

FIG. 15. Time histories of Freon crust thickness (Δ_f) and ice melt layer thickness (Δ_w).

The crust and melt layer thickness–time curves are shown in Fig. 15 for the Freon 112A-ice wall system. One notes that $\Delta_f(\tau)$ passes through a maximum value $\Delta_{f,\max} = 0.86$ at a dimensionless time $\tau \simeq 4.0$. At this extremum, the heat flux coming from the flowing liquid is equal to that removed through the ice melt by conduction. The rate of Freon solidification passes through a stage of zero speed and Freon crust melting begins. The Freon crust lifetime $\tau_{life} = 49.0$. The ice melt layer thickness increases with time and reaches $\Delta_w = 1.21$ at $\tau = \tau_{life}$. Assuming the local convective heat-transfer coefficient in the Freon flow is given by the constant Stanton number formula, $h = Ac_f\rho_f u$, we can convert these dimensionless numbers to predicted maximum Freon crust thickness $\delta_{f,\max}$, Freon crust lifetime t_{life} and ice melt layer thickness $\delta_{w,\max}$ at $t = t_{life}$. For the experimental conditions leading to a local Freon velocity of $\sim 500\,\mathrm{cm\,s^{-1}}$, we obtain $h = 0.2\,\mathrm{cal\,cm^2\,s^{-1}}$. This leads to the inferences $\delta_{f,\max} \sim 1.85 \times 10^{-3}\,\mathrm{cm}$, $\delta_{w,\max} = 1.1 \times 10^{-2}\,\mathrm{cm}$, and $t_{life} \sim 0.2\,\mathrm{s}$ for a Freon stream at 70°C. It is clear that assumptions 3 and 4 of Section 5 are readily satisfied. However, assumption 4 becomes increasingly difficult to satisfy for low Freon flow velocities and temperatures. For velocities of the order $100\,\mathrm{cm\,s^{-1}}$ and Freon temperatures of about 45°C, we predict a Freon crust lifetime of $\sim 200\,\mathrm{s}$. The quasi-steady ice melting model described in Section 5 breaks down under these conditions since t_{life} is very much greater than the injection period.

TRANSFERT THERMIQUE POUR UN ECOULEMENT DANS UN TUBE LORS D'UNE SOLIDIFICATION ET D'UNE FUSION

Résumé—On considère le transfert thermique au cours de la solidification d'un liquide en écoulement et de la fusion de la paroi. En particulier, on étudie expérimentalement un écoulement turbulent de Fréon 112 A chaud (point d'ébullition 40,5°C) à travers un tube épais de glace. L'attention est portée sur l'attaque de fusion de la glace par le Fréon. On étudie les effets de la pression d'injection du Fréon et de la température sur la quantité de glace fondue collectée à la sortie du tube pour une période d'injection fixée. La forme du canal de glace en fusion en fonction du temps, de la pression d'injection et de la température du Fréon est déterminée à partir de la prise de Fréon gelé qui demeure dans le tuyau de glace. On compare des résultats numériques basés sur un modèle simple de fusion quasi stationnaire avec les résultats expérimentaux. Le modèle représente les mesures raisonnablement bien pour des températures de Fréon supérieures à 70°C, ce qui montrerait que les processus de fusion pariétale de la glace est controlée par la croissance et la disparition des couches de Fréon gelé sur la paroi du tube de glace.

GEFRIERENDE-SCHMELZENDE WÄRMEÜBERTRAGUNG IN EINER ROHRSTRÖMUNG

Zusammenfassung— Es wird ein Wärmeübertragungsproblem behandelt, bei dem eine strömende Flüssigkeit an einer schmelzenden Wand gefriert. Im vorliegenden Fall wurde eine experimentelle Untersuchung durchgeführt, bei der eine turbulente Strömung von warmem Freon 112A (Schmelzpunkt: 40, 5°C) durch ein Rohr aus dickem Eis fließt. Es wurden die Einflüsse untersucht, die der Einspritzdruck und die Temperatur des Freons auf die Menge des in einer bestimmten Zeitspanne verflüssigten Eises am Rohrausgang haben. Die Form des geschmolzenen Eiskanals als Funktion der Zeit, des Einspritzdrucks und die Freon-Temperatur wurden über die gefrorenen "Freon-Gußteile", die im Eisrohr verblieben, ermittelt. Die über ein einfaches, quasi-stationäres Schmelzmodell berechneten numerischen Ergebnisse wurden mit den experimentellen Schmelzergebnissen verglichen. Das Modell gab die Messungen für Freon-Temperaturen über 70°C recht gut wieder, woraus ersichtlich ist, daß der Prozeß des Eisschmelzens durch Wachstum und Abnahme der gefrorenen Freon-Schichten auf der Eiswand des Rohres bestimmt wird.

ТЕПЛОПЕРЕНОС ПРИ ТЕЧЕНИИ ЗАТВЕРДЕВАЮЩЕЙ ЖИДКОСТИ В ТРУБЕ С ПЛАВЯЩИМИСЯ СТЕНКАМИ

Аннотация — Рассматривается перенос тепла при затвердевании жидкости, натекающей на плавящуюся стенку. В частности, выполнено экспериментальное исследование турбулентного течения нагретого Фреона 112 А (точка плавления 40,5°С) в толстостенной трубке из льда. Особое внимание уделялось плавлению стенки в результате действия на неё потока фреона. Исследовалось влияние как давления при подаче фреона, так и температуры на интенсивность таяния льда путём измерения количества жидкости на выходе из трубы за определенный промежуток времени. По замёрзшей в ледяной трубке фреоновой «отливке» определялась конфигурация деляного канала в зависимости от времени, давления и температуры фреона. Численные результаты, найденные с помощью простой квазистационарной модели плавления, сравнивались с экспериментально полученными данными по таянию льда. Установлено, что модель хорошо описывает процесс при температуре фреона выше 70°С. Это свидетельствует о том, что процесс плавления стенки ледяной трубки определяется ростом и распадом на ней слоёв замерзшего фреона.